Behavioral/Systems/Cognitive

Ketamine–Xylazine-Induced Slow (<1.5 Hz) Oscillations in the Rat Piriform (Olfactory) Cortex Are Functionally Correlated with Respiration

Alfredo Fontanini,[1,2] **PierFranco Spano,**[2] **and James M. Bower**[3]

[1]Division of Biology, California Institute of Technology, Pasadena, California 91125, [2]Division of Pharmacology, Department of Biomedical Sciences and Biotechnology, Brescia University Medical School, 25123 Brescia, Italy, and [3]Research Imaging Center, University of Texas Health Science Center at San Antonio, and Cajal Neuroscience Center, University of Texas San Antonio, San Antonio, Texas 78284-6240

The occurrence of low frequency (<1.5 Hz) cerebral cortical oscillations during slow-wave sleep has recently lead to the suggestion that this pattern of activity is specifically associated with conditions in which the brain is mostly closed to external inputs and running on its own. In the current experiments, we used a combination of *in vivo* intracellular and extracellular field potential recordings obtained under conditions of ketamine–xylazine anesthesia to examine slow-wave behavior in the olfactory system. We demonstrate the occurrence of low-frequency oscillations in field potentials of both the olfactory bulb and cortex and in the membrane potentials of cortical pyramidal cells. By monitoring ongoing breathing, we also show that these oscillations are all correlated with the natural breathing cycle. Using a tracheotomized preparation, we demonstrate that slow oscillatory patterns could occasionally be produced even when air is no longer entering the nose, supporting the view that the olfactory system has an intrinsic propensity to oscillate. However, in the case of tracheotomized rats, the amplitude and regularity of the oscillations as well as their patterns of correlation are disrupted. All temporal relationships were restored when air was pulsed into the nostrils. We conclude that, in the olfactory system of freely breathing rats, there is a strong relationship between the occurrence and timing of slow oscillations and the ongoing periodic sensory input resulting from respiration. This coupling between olfactory cortex slow oscillations and respiration may result from the interaction between respiratory-related rhythmic input and the tendency for olfactory structures to oscillate intrinsically. We believe this finding has important functional as well as evolutionary implications.

Key words: **piriform cortex; olfactory cortex; olfactory bulb; slow oscillations; respiration; ketamine; rat**

Introduction

Although it has been known for many years that the nervous system generates oscillatory behavior in a wide range of frequencies (Adrian, 1942; Bremer, 1958; Freeman, 1960), the functional significance of this dynamical behavior has recently become a growing focus for many physiologists (Wehr and Laurent, 1996; Buzsaki, 1998; Engel et al., 2001), modelers, and theorists (Hopfield, 1995; Traub et al., 1999; Freeman, 2000; Hasselmo et al., 2000; Destexhe and Sejnowski, 2001). Central in many interpretations of the functional significance of cerebral cortical oscillatory behavior is the question of the origins of this behavior and, in particular, its relationship to ongoing afferent input (Eckhorn et al., 1988; Gray et al., 1989).

In this study, we analyzed the effects of afferent input on oscillations in the olfactory system occurring at frequencies lower than 1.5 Hz. These low-frequency oscillations have been recorded in rats under conditions of ketamine–xylazine anesthesia, comparable with those used by Steriade and colleagues to study slow oscillations in neocortex (Steriade et al., 1993a,b). On the basis of similarities between the neocortical oscillations and those seen during slow-wave sleep (Steriade et al., 2001), it has been proposed that these slow oscillations reflect a behavioral condition in which the brain is mostly closed to the external environment and running on its own (Timofeev et al., 1996a; Steriade, 2000; Destexhe and Sejnowski, 2001). This assertion is consistent with electrophysiological results demonstrating slow-wave oscillations in deafferented neocortical slices (Sanchez-Vives and McCormick, 2000) and slabs (Timofeev et al., 2000).

Using combined simultaneous *in vivo* intracellular and extracellular recording techniques, we demonstrate the presence of ketamine–xylazine-induced slow oscillations in local field potentials in the olfactory bulb (OB) and piriform cortex (PC) as well as in pyramidal cell membrane potentials in the piriform cortex. Furthermore, we show that these oscillations are correlated with the natural breathing cycle of the rat and therefore appear to be directly related to ongoing periodic patterns of afferent input linked to respiration. Supporting this interpretation, we demonstrate that both the amplitude and regularity of these oscillations are reduced in tracheotomized preparations when air is no longer entering the nose. The temporal relationship between extracellu-

Received March 19, 2003; revised July 8, 2003; accepted July 9, 2003.

This work was supported by a Multidiciplinary University Research Initiative grant managed by the Army Research Office. We thank Drs. Marco DeCurtis and Arianna Maffei for helpful comments on this manuscript.

Correspondence should be addressed to Alfredo Fontanini, Department of Biology, MS 008, Brandeis University, 415 South Street, Waltham, MA 02454. E-mail: alfredof@brandeis.edu.

 0270-6474/03/237993-09$15.00/0

lar and intracellular recordings also changes under these conditions. Pulsing air into the nostrils not only restores the oscillations and the temporal relationships but also directly entrains their frequency. On the basis of this data, we conclude that, in freely breathing rats, there is a strong relationship between slow oscillations in the olfactory bulb and cortex and the ongoing periodic sensory input resulting from respiration, almost certainly interacting with an intrinsic tendency for olfactory structures to oscillate (Bower, 1995). The conclusion that respiration is reflected in the temporal behavior of the olfactory system is consistent with previous studies on the piriform cortex (Wilson, 1998) and olfactory bulb of rats (Macrides and Chorover, 1972; Chaput et al., 1992; Sobel and Tank, 1993) and with recent imaging results in humans (Sobel et al., 1998). This work was first presented in abstract form (Fontanini et al., 2001).

Materials and Methods

Animal surgery. All animal procedures were approved in advance by the Animal Use Committee of the California Institute of Technology. Adult Sprague Dawley rats (250–300 gm) were anesthetized with ketamine–xylazine (100 mg/kg, 5 mg/kg, i.p.) and mounted on a stereotaxic frame (Kopf Instruments, Tujunga, CA). Heart rate and body temperature were monitored throughout the experiment, and body temperature was maintained constant (36 ± 1°C) using a custom designed biofeedback system. The general level of anesthesia was maintained so that hindlimb pinching produced no reflex movement. When necessary, an additional dose (30% of initial dosage) of ketamine–xylazine was injected intraperitoneally. Xylocaine was applied topically at the edge of all incisions and at pressure points to minimize pain. After exposure of the skull, burr holes were drilled in its dorsal part above the olfactory bulb, lateral olfactory tract, and anterior piriform cortex, and the dura mater was carefully removed and the brain was covered with mineral oil to prevent drying. The cisterna magna was widely incised, and the cerebrospinal fluid was drained to minimize brain pulsation. In 13 rats, tracheotomy was performed, and a small tubing was inserted in the nostril ipsilateral to the recording site. In these experiments, puffs of clean filtered air were injected into the right nostril using a picospritzer. The duration of the pulse was 100 msec, and the pressure varied between 45 and 55 psi. This stimulus was strong enough to be detected on the finger of the experimenter and capable of moving the rats' whiskers at a distance of 4–5 mm. In preliminary experiments, air puffs at 20 psi were shown to have no influence on neuronal activity. Respiration was monitored by recording the chest wall movements using a piezoelectric device.

Extracellular field potential recordings and electrical stimulation. Extracellular field potential recordings and electrical stimulation were both accomplished using unipolar tungsten electrodes (MicroProbe, Potomac, MD) with a resistance of 1 MΩ. Stimulating and extracellular recording electrodes were placed in the olfactory bulb, lateral olfactory tract, and piriform cortex by relying on stereotaxic coordinates relative to bregma (olfactory bulb: 7–8 mm anterior (AP), 1–2 mm lateral (ML), 1–2 mm ventral (DV); piriform cortex: 0.5–1.5 mm AP, 4–5 mm ML, 6–7 mm DV; lateral olfactory tract: 3 mm AP, 3.5 mm ML, 4.5–5 mm DV) (Paxinos and Watson, 1997). Recording electrodes were positioned in the granule cell layer of the olfactory bulb and in layer I of the piriform cortex. Positioning accuracy for stimulation and recording was determined by testing to assure that stimulating electrodes produced the characteristic biphasic electrophysiological response to strong lateral olfactory tract stimulation (see Fig. 1*A*,*B*) (Haberly, 1973; Ketchum and Haberly, 1993; Stripling and Patneau, 1999). Extracellular signals were filtered (0.1–5 KHz) and amplified with an extracellular amplifier (A-M Systems, Carlsborg, WA).

Intracellular recordings. Intracellular recordings in piriform cortex were obtained using sharp electrodes pulled with a horizontal puller (P87; Sutter Instruments, Novato, CA) from borosilicate glass (1 mm o.d., 0.58 mm i.d.) (A-M Systems). Recording electrodes with impedance ranging between 40 and 70 MΩ were filled with 3 M potassium acetate. Electrodes were slowly (~100 μm/min) lowered dorsally with a hydraulic micropositioner (Kopf Instruments) using field potential responses to lateral olfactory tract stimulation to determine when the electrode tip reached layers II/III of the piriform cortex (usually ~6 mm ventral from the brain surface). Recordings were performed in bridge-balance mode using an Axoclamp 2-A intracellular amplifier (Axon Instruments, Union City, CA). After impalement, a hyperpolarizing bias current (0.5–2 nA) was injected to stabilize the membrane potential of the cell. Once the cell activity reached a stable state, the current was discontinued. Neurons included in this study were required to maintain spontaneous membrane potentials more negative than −60 mV with regenerative action potentials with an amplitude that exceeded 50 mV. In addition, all recorded neurons responded to stimulation of the lateral olfactory tract with the biphasic response (see Fig. 1*C*) characteristic of cells identified as pyramidal type with intracellular labeling techniques, as reported previously (Haberly and Bower, 1984). Respiratory activity and intracellular and extracellular data were simultaneously acquired at 20 kHz with a Digidata 1200 board (Axon Instruments) connected to a personal computer running Clampex 8 acquisition software (Axon Instruments).

Data analysis. Fifteen to sixty second long traces were used for analysis. To allow a faster processing of data, the sampling rate was reduced offline from 20 to 2 kHz using the decimation algorithm implemented in Clampfit 8 (Axon Instruments). This procedure consisted of copying to the output data record the first point of every *n* points (where *n* is the reduction factor; in our case, 10) for each signal. To be sure that signals were not filtered in the frequency domain, we compared a fast Fourier transform (FFT) performed on the data before and after decimation; the result showed no distortion at low frequencies. Also, a comparison of the traces before and after decimation was performed to test for no distortion in the time domain.

Histograms of membrane potentials. Membrane potential histograms were constructed using 30 sec data traces binned at 2 mV. The experimental histogram was then fitted with a Lavenberg–Marquard algorithm using a sum of two Gaussians as follows:

$$a1 \cdot \exp(-[(x - b1)/c1]\text{^}2) + a2 \cdot \exp(-[(x - b2)/c2]\text{^}2),$$

where $b1$ and $b2$ represent the mean of the two Gaussians.

Spectral analysis. Power spectral density was estimated using Welch's averaged periodogram method. Traces were divided into ~15 sec windows with a 50% overlap and analyzed with a 32768 points FFT. These parameters allowed us to achieve a resolution of 0.06 Hz, which was critical for investigating, in the different signals, the coincidence of the peak at low frequencies.

Cross-covariance analysis. The correlation between the membrane potential of the piriform cortex pyramidal cell and local field potentials in either the layer I of the piriform cortex or the granular layer of the olfactory bulb was obtained by computing the cross-covariance (cross-correlation normalized by the mean) between 15 and 30 sec recordings of intracellular neuronal membrane potentials and local extracellular field potentials. Positive or negative peaks of the cross-covariance were computed within 0.5 and −0.5 sec lags. The correlation between the membrane potential and respiratory activity was also investigated by estimating the respiratory wave-triggered average. In brief, a breathing cycle (from the beginning of one inspiration to the beginning of the next) was divided into eight bins, and the average membrane potential was computed within each bin. We repeated this operation for every breathing cycle in a ~30 sec recording, and the average membrane potential for each of the eight bins was then averaged across all of the respiratory cycles. Data analysis was performed using Matlab (Mathworks, Natick, MA).

Histology. After termination of the experiment, an electrolytic lesion (100 μA; 5–10 sec) was made to verify the proper positioning of all recording and stimulation electrodes (see Fig. 1). The rat was then deeply anesthetized (Nembutal, 1 ml, i.p.) and transcardiacally perfused with saline solution followed by 3% paraformaldeyde. The brain was removed, stored in 3% paraformaldeyde for at least 2 d, and sliced with a vibratome (thickness, 200 μm). Lesions were revealed with cresyl violet staining using standard procedures.

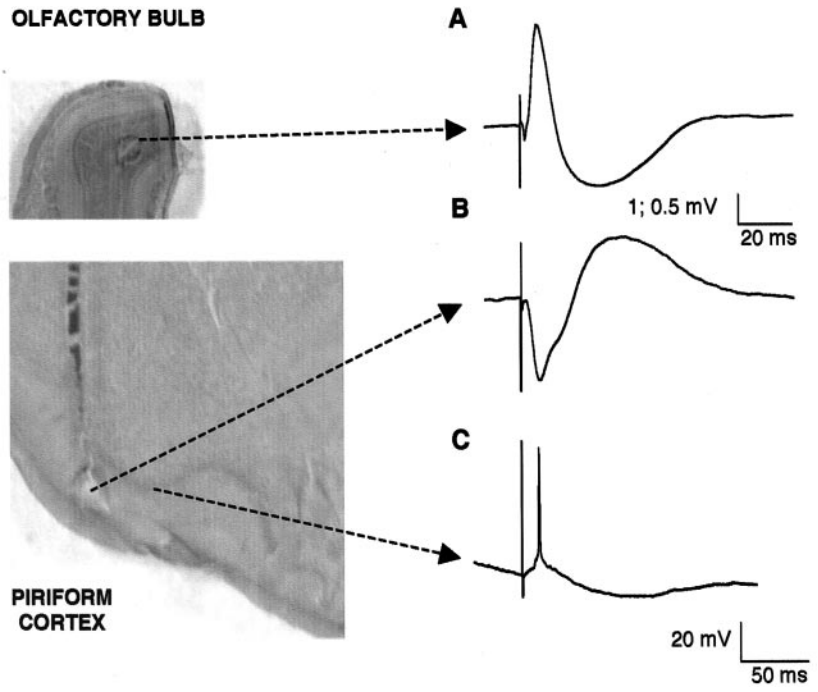

Figure 1. Positioning of electrodes: characteristic response to LOT strong electrical shock. *A*, Extracellular recording from the granule cell layer of the olfactory bulb. *B*, Extracellular recording from layer I of the piriform cortex showing the monosynaptic and disynaptic (associative) components characteristic of that layer. *C*, Characteristic intracellular response of a layer II/III pyramidal neuron to LOT stimulation with an EPSP or spike followed by a prolonged hyperpolarization. Calibration: 1 and 0.5 mV, 20 msec (from olfactory bulb and piriform cortex, respectively); 20 mV, 50 msec for intracellular recordings. Left, Histological assessment of extracellular electrode positioning. Note that lesions in the granule cell layer of the olfactory bulb (top) and in layer I of the piriform cortex (bottom) are shown. Arrows connect areas in which recordings were performed to their characteristic response.

Results

Recordings

We report here the results of a total of 40 individually recorded neurons obtained in 34 rats. These neurons were judged most likely to be pyramidal cells because of the fact that recordings were obtained at a depth in which lateral olfactory tract (LOT) stimulation induced both extracellular field potential responses typical of layer II/III and intracellular responses typical of pyramidal cells (Fig. 1*C*). All intracellular recordings were accompanied by extracellular field potential recordings obtained from the olfactory bulb and cortex.

Periodic variations in membrane potential

Figure 2*A* shows the pattern of membrane potential behavior characteristic of all neurons intracellularly recorded in freely breathing rats under the ketamine–xylazine anesthesia used in these experiments. As shown, membrane potentials exhibited large 0.7–1.5 Hz periodic fluctuations that seldom resulted in action potential generation. Taken as a whole, the average membrane potential for the recorded neurons was -81.85 ± 5.72 mV ($n = 20$); however, as shown in the histogram in Figure 2*B*, the periodic variations in membrane potential result in a bimodal distribution of instantaneous membrane voltage. When this bimodal distribution is fitted by a sum of two Gaussians, the mean value of the membrane potential during the "up state" is -76.08 ± 5.28 mV ($n = 16$), whereas the mean value is -89.54 ± 6.1 mV ($n = 16$) for the "down state."

The mean width of these slow periodicities is 13.45 ± 5.04 mV ($n = 16$), and the power of the peak at the power spectral density is 270.66 ± 213.45 mV^2/Hz ($n = 18$). As shown in Figure 2*C*, occasionally in some cells ($n = 5$), this ongoing periodic pattern of activity was interrupted for short periods (usually shorter than 10 sec) of a steady, more depolarized membrane potential that was often accompanied by action potential generation. These short periods of steady membrane depolarization subsequently returned to the more hyperpolarized, large amplitude periodic behavior.

Relationship between membrane periodicity and other measures of periodicity in the olfactory system

Given the similarity between the membrane periodicities reported here and those suggested by Steriade and colleagues to be characteristic of the relatively sensory deafferented condition of slow-wave sleep (Steriade et al., 1993a,b), we elected to look more closely at the relationship between these membrane fluctuations and periodic patterns of sensory activity in the olfactory system. It is well known that the olfactory bulb, which provides the primary afferent projection to the piriform cortex, shows periodic activity (Bressler and Freeman, 1980; Bressler, 1984), and that the sniffing activity of rats is rhythmic as well (Macrides and Chorover, 1972; Bhalla and Bower, 1997).

The data shown in Figure 3*A* compare pyramidal cell membrane potential (V_m) recordings with those obtained with extracellular electrodes in the PC and OB. The bottom trace in Figure 3*A* was obtained from a body cuff measuring ongoing extension and contraction of the chest associated with respiration. All four traces were recorded simultaneously. Visual inspection of the raw data obtained with these four types of recordings indicates similar slow-wave periodicities in each trace. This is quantified in the power spectral analysis (Fig. 3*B*--*E*), which demonstrates peaks between 0.7 and 1.5 Hz in recordings of membrane voltage (Fig. 3*B*), field potentials in the piriform cortex (Fig. 3*C*), and olfactory bulb (Fig. 3*D*), as well as in the animal's ongoing respiration (Fig. 3*E*). The average peak frequency is 0.97 ± 0.13 Hz ($n = 18$) for all signals.

Correlations in periodic behavior

In addition to similarities in slow-wave behavior, visual inspection suggests both strong correlations and consistent phase relationships in the periodic behavior seen in these records (Fig. 3*A*, dotted box). These temporal relationships were confirmed using cross-covariance analysis (Fig. 3*F*--*G*). Figure 3*F* indicates that the depolarized component of the intracellularly recorded membrane potential is strongly associated with the negative deflection of layer I local field potential in the piriform cortex. When assessed using the negative peak of the cross-covariance within a ± 0.5 sec time lag (Fig. 3*F*, asterisk), the peak correlation value was found to be -0.55 ± 0.17 ($n = 17$). The average lag of the peak between membrane potential and cortical local field potential was only 0.002 ± 0.07 sec ($n = 17$). There was also a strong correlation between the local field potential recorded in the granule cell layer of the olfactory bulb and the pyramidal cell membrane potential. Assessing the positive peak within a ± 0.5 sec of the cross-covariance between membrane potential and local field

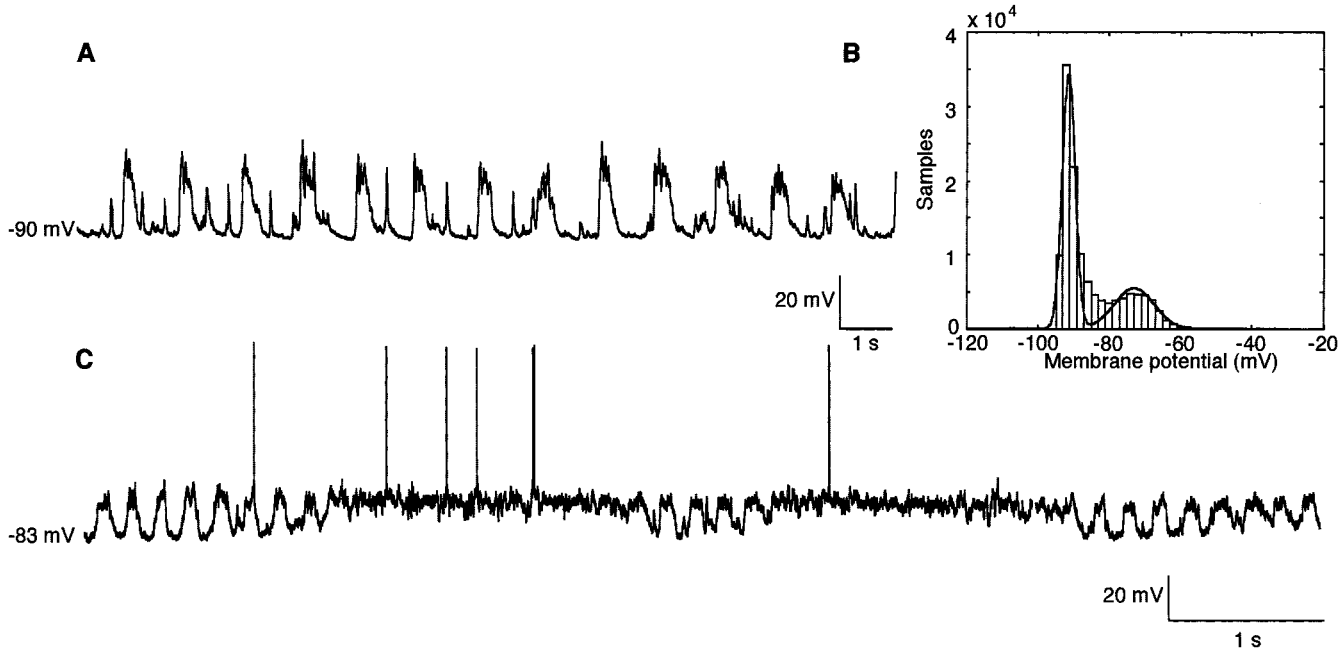

Figure 2. Characteristic ongoing membrane potential fluctuations in layer II/III pyramidal cells. *A*, Membrane potential recording from a representative neuron; the spiky events occurring in the down states are PSP spontaneously generated. *B*, Bimodal distribution of the histogram of membrane potential in a slowly oscillating cell: fitting with a sum of two Gaussians (continuous line). *C*, An example of less frequently seen behavior in which ongoing slow-wave oscillations were occasionally interrupted by periods of sustained membrane depolarization and accompanying action potential generation.

potentials recorded in the olfactory bulb (Fig. 3*F*, asterisk), a correlation with peak value 0.44 ± 0.14 ($n = 17$) was found. In the case of the olfactory bulb, the membrane potential depolarization was correlated with the positive deflection of the olfactory bulb field potential with a lag of 0.13 ± 0.05 sec ($n = 17$).

The raw data in Figure 3*A* also suggest a regular phase relationship between membrane potential and ongoing respiration. This is quantified in Figure 3*H*, in which the phase of respiration is plotted against the mean membrane potential during eight phases of the breathing cycle. The zero phase in this plot corresponds to the start of inhalation (i.e., minimum circumference of the diaphragm). The results show, at least in freely breathing rats, a consistent and strong relationship of pyramidal cell membrane potential on the respiratory cycle during periods of slow oscillations, with the largest amplitude membrane potential occurring at a lag of 225–315°. Membrane potential is essentially flat for the first 180° in the cycle.

Effect of tracheotomy on membrane potential slow oscillations

The analysis shown in Figure 3 suggests that the slow periodicity seen in membrane potentials, as well as in the olfactory bulb and piriform cortex, could be directly related to some feature of the periodic breathing of the rat. To determine whether the neuronal periodicity was related to the act of breathing or the actual passage of air into the nostrils, in several animals, all four physiological measures were obtained after tracheotomy. In tracheotomized animals, air flows directly into the trachea without passing through the nostrils.

Figure 4 shows variations in the pattern of membrane potentials recorded in the tracheotomized rats. Under these conditions, we found a higher degree of variability in the pattern of membrane fluctuations in the same cell. All 13 recorded cells generated periods of spontaneous slow fluctuations with little or no spiking activity (Fig. 4*A*) similar to those seen in the intact preparation (Fig. 2*A*). However, in the intact preparation, this pattern of activity is generally sustained for much longer periods (on the order of minutes) than is the case in tracheotomized rats (typically only 10–30 sec). Tracheotomized rats also had a reduction in the amplitude of slow membrane potential fluctuations with the average SDs being 3.43 ± 1.21 mV ($n = 13$) versus 6.44 ± 2.37 mV ($n = 20$; $p < 0.001$) in the case of intact preparation. Patterns of slow oscillations in these rats alternated with periods of hyperpolarized membrane potential (Fig. 4*B*) as well as the depolarized potential also seen in intact animals (Fig. 4*C*). Given the focus of this paper on slow oscillations, analysis of responses in the tracheotomized animals was restricted to times when membrane potentials showed slow oscillations similar to those seen in intact preparations.

Figure 5*A* compares Vm, local field potentials in the PC and OB, and the respiratory rhythm recorded during a period of slow oscillations in a tracheotomized preparation. Note that while air was not flowing through the nasal epithelium, the animal was still controlling its own breathing in these experiments. The records shown in Figure 5*A* clearly indicate that intracellular membrane potential continues to be periodic, as does the activity seen with extracellular field potentials in the piriform cortex, olfactory bulb, and of course respiration. However, whereas all four measures show periodicities, there are clear differences between tracheotomized and intact rats (Fig. 3) in the power spectral analysis of the data (Fig. 5*B--E*). The average peak value of the power spectral density for membrane potential is 37.08 ± 75.43 mV^2/Hz ($n = 13$), which is lower than in the intact animal at 270.66 ± 213.45 mV^2/Hz ($n = 20$; $p < 0.0001$). Moreover, the main oscillatory frequency is less narrowly peaked (see Fig. 3*B* for comparison) and is also centered at a lower frequency than in the intact case; the average peak frequency is 0.80 ± 0.27 Hz ($n = 13$) for the membrane potential, 0.75 ± 0.25 Hz ($n = 13$) for local

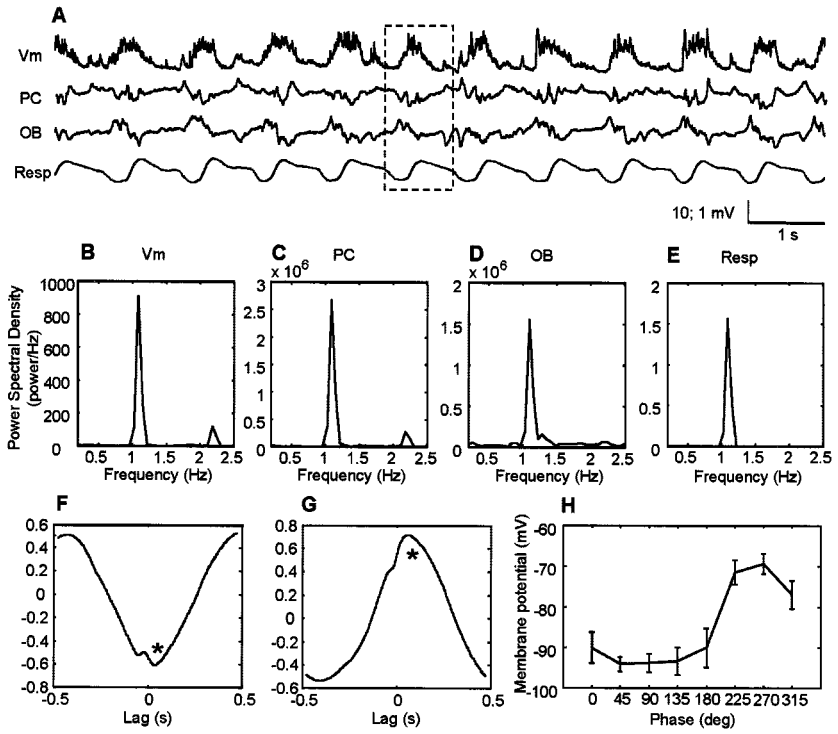

Figure 3. Comparisons of cortical, bulbar, and respiratory oscillations. *A*, Representative raw traces of pyramidal cell membrane potential (Vm), local field potentials in layer I of PC, in the granule cell layer of the OB and respiratory wave as recorded from chest wall movements (Resp). In the respiratory wave, the downward deflection represents the inspiration. All traces were recorded simultaneously. The dotted line highlights a single hyperpolarization-depolarization cycle. The vertical scale for the intracellular records is 10 mV, whereas the extracellular records are 1 mV. The graphs *B--E* indicate the power spectral density for the recorded membrane potentials (*B*), local field potentials recorded in the piriform cortex (*C*), in the olfactory bulb (*D*), and ongoing respiration (*E*). *F*, Representative cross-covariance between membrane potential of a layer II/III pyramidal cell and layer I olfactory cortex local field potentials. Note that the negative peak (asterisk) at a time close to 0 sec is shown; such a negative peak reflects the anticorrelation existing between membrane potential and local field potentials in layer I of the piriform cortex. *G*, Representative cross-covariance between membrane potential and local field potentials in the granule cell layer of the olfactory bulb. In this case, the peak near time 0 is positive, consistent with the positive correlation between membrane potential and field potentials in the olfactory bulb. *H*, Respiratory wave-triggered average of membrane potential; 0° phase represents the beginning of the inspiration.

field potentials in the olfactory cortex, and 0.81 ± 0.35 Hz (n = 13) for local field potentials in the olfactory bulb. The average respiratory frequency in tracheotomized rats is similar to that in intact rats: 0.99 ± 0.10 Hz (n = 13) and 0.97 ± 0.13 Hz (n = 20), respectively.

Comparison of the traces shown in Figure 5*A* with those in the intact animal (Fig. 3*A*) also indicates clear changes in the relationships between the periodic behavior seen in the olfactory system. This is shown in Figure 5, *F* and *G*, which superimposes cross-covariance analysis in the intact animal (dashed lines) with those performed in exactly the same manner for the tracheotomized rats. These comparisons show that although there continues to be a strong correlation between membrane potential and local cortical (Fig. 5*F*) and bulbar (Fig. 5*G*) extracellular potentials, the phase relationships are completely different. In both cases, there is a shift in correlation of almost 180° after tracheotomy. Thus, in the piriform cortex, the intracellular depolarization is now associated with a positive deflection in the cortical local field potentials, and the peak near 0 sec lag of the cross-covariance is now positive (0.61 ± 0.14; n = 13). In the case of the olfactory bulb, the intracellular depolarization is now associated with the negative deflection of the local field potential, and consistently the peak near 0 sec lag of the cross-covariance is negative (−0.70 ± 0.09; n = 13). These changes were seen in all 13 cells recorded under tracheotomized conditions.

Effects of respiration on intracellular slow oscillations

The original intent in examining responses in the tracheotomized animal was to determine the influence of respiration itself on the periodicities seen in the olfactory system. Figure 5*H* shows comparisons made between the membrane potential and phase of respiration in each condition (dashed line, intact preparation). These data clearly indicate that the periodic behavior of the olfactory system is not dependent on respiration in the tracheotomized rats. This result suggests that the correlation seen between respiration and neural oscillations in the olfactory system of intact rats is related to the influx of air into the nasal cavity.

To conclusively demonstrate this hypothesis, we conducted several experiments in which air was pressure injected into the nostrils of tracheotomized rats. The results are shown in Figure 6. Injection of air in tracheotomized rats produced regular and sustained slow membrane potential fluctuations lasting as long as the air-puff injection continued. Furthermore, the frequency of the slow oscillations could be directly controlled by the frequency of the air puff. Thus, air puffs at ~0.5 Hz (Fig. 6*A*), ~1 Hz (Fig. 6*B*), and ~2 Hz (Fig. 6*C*) produced oscillations with corresponding frequencies. The lines under each trace indicate the onset of the air puff and clearly show a temporal relationship between the onset of the air puff and depolarization of cell membrane potential. This result is also reflected in the power spectral analysis data after each set of traces (Fig. 6*D--F*). The peaks of power spectral density were always narrow and occurred at the same frequency at which the air was puffed into the nostrils.

Finally, Figure 7 examines the correlation between Vm and extracellular recordings in the PC and OB in tracheotomized animals receiving air-puff stimuli. Data obtained at a ~1 Hz stimulus frequency are shown, although data at the other two frequencies were similar. The results show that air-puff stimulation returns the patterns of correlation to those seen in the intact animal (Fig. 3, compare *F* and *G*). The plot of the cross-covariance between membrane potential and cortical local field potentials (Fig. 7*B*) shows that the two signals are anticorrelated (value of the negative peak, −0.49 ± 0.10; n = 10). The plot in Figure 7*C* displays the cross-covariance between membrane potential and local field potentials in the olfactory bulb; in this case, the actual shape of the correlation differs somewhat from the intact preparation but still includes a large phase-delayed positive peak.

Discussion

Slow (<1.5 Hz) oscillations in the olfactory system

The results presented here demonstrate for the first time the presence of slow (<1.5 Hz) respiratory-related oscillations in the

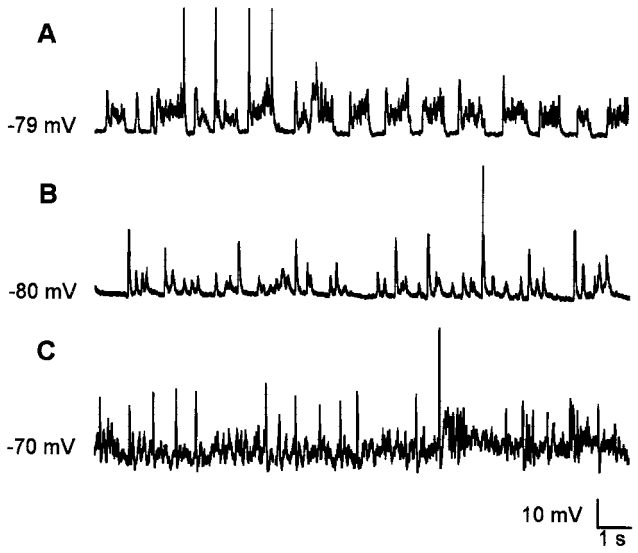

Figure 4. Patterns of intracellular activity in tracheotomized rats. *A*, Slow oscillations in absence of rhythmic respiratory input. *B*, Hyperpolarized membrane potential with large synaptic potentials. *C*, Depolarized membrane potential with high-frequency, low-amplitude oscillations.

olfactory system under conditions of ketamine–xylazine anesthesia. This study is also the first to examine the relationship between slow olfactory field potential oscillations, intracellular membrane potential, and respiratory activity.

Phase coupling within the olfactory system

Intracellular slow oscillations appeared to be highly correlated with extracellular field potentials recorded at a distance of ~1–2 mm; this observation indicates a high degree of synchrony of slow oscillations within the olfactory cortex. Cortical slow oscillations were also found to be strongly correlated with bulbar activity, again suggesting a high level of phase coupling in the whole olfactory bulb–olfactory cortex system. This observation allows us to draw an analogy between the olfactory system and the thalamocortical system. In fact, as in the case of the olfactory cortex, neocortical slow oscillations are strongly correlated among wide cortical areas (Destexhe et al., 1999) and with the thalamus (Timofeev and Steriade, 1996b). The main difference between these two systems is in the genesis of these oscillatory patterns. In the thalamocortical system, slow oscillations are generated within the cortex and reverberated in a thalamocortical loop (Bazhenov et al., 2002); our data support the view that in the bulbar-cortical system, slow oscillations are generated by barrages of synaptic inputs rhythmically activating the olfactory bulb and propagating in the cortex. Of course, our data cannot exclude the possibility that feedback projections from the olfactory cortex to the olfactory bulb may play a role in the genesis or maintenance of this oscillatory pattern.

Relationship of slow-wave oscillations to afferent input

Steriade and colleagues proposed that the presence of these slow oscillations reflects a behavioral condition in which the brain is mostly closed to the external environment and running on its own (Timofeev et al., 1996a; Steriade 2000). Electrophysiological results demonstrate slow-wave oscillations in neocortical slices (Sanchez-Vives and McCormick, 2000) and slabs (Timofeev et al., 2000), supporting Steriade's proposal that slow-wave oscillations are a specific indication of an isolated deafferented state.

The results of this study demonstrate that this is clearly not the case in the olfactory system. The respiratory wave-triggered average of intracellular recordings in the olfactory cortex demonstrates a strong relationship between the timing of respiration and cortical slow oscillations. Furthermore, the occurrence of slow oscillations, similar to those observed in freely breathing rats, is modified when airflow through the nostrils is removed by tracheotomy. After tracheotomy, membrane potentials in piriform cortex pyramidal cells become more variable; when present, periods of slow oscillation have shorter duration, smaller amplitudes, no correlation with respiration, and reversed cross-covariance patterns. Slow oscillations similar to those occurring in the intact preparation were then reestablished when air was forced in the nostrils independent of the rat's breathing cycle. Under these conditions, the frequency of membrane potential oscillations followed the frequency of air stimulation. Therefore, at least under ketamine anesthesia, the timing and to some extent the occurrence of slow oscillations in the olfactory system appear to be directly related to the flow of air into the nostrils. Our data are consistent with previous intracellular recordings in the piriform cortex of urethane-anesthetized rats (Wilson, 1998), showing a correlation between membrane potential fluctuations and phase of respiration. Under urethane anesthesia, however, spontaneous membrane potential fluctuations appeared to be faster, consistent with a higher respiratory frequency with such anesthetic, and to have lower amplitude. Our results are also consistent with recent imaging studies in humans showing a direct correlation between breathing and activity in the olfactory cortex (Sobel et al., 1998). Of course, the particular frequencies of slow wave and respiratory rhythms are likely to differ, depending on the species involved (Achermann and Borbély, 1997; Amzica and Steriade, 1997).

What input is responsible for this correlation?

Our finding that air puffed into the nostrils of a tracheotomized rat correlates bulbar and cortical activity leaves open the question as to what specific neural signal is responsible. The fact that respiratory movement of the diaphragm is not correlated with neural activity in the tracheotomized rat indicates that the signal is not paced by ascending signals coming from bulbar respiratory centers. Instead, the neuronal correlation appears to be directly related to the movement of air into the nostrils.

Air moving into the nostrils influences several different sensory afferent systems, which could in turn influence bulbar and cortical activitiy. First, recordings from primary olfactory sensory neurons clearly show a correlation between neural activity in the olfactory epithelium and breathing (Chaput, 2000). Second, it is known that the there are pressure detectors in the walls of the nasal cavity that also respond periodically during inhalation (Tsubone, 1990). Additional studies will be necessary to determine which or what combination of this sensory information is responsible for the observed correlations. Again, however, the data makes it clear that these correlations are dependent on some form of sensory input resulting from entry or air into the nostrils.

Interestingly, in some instances, the slow oscillatory pattern was disrupted, and slow oscillations were replaced by high-frequency, low-amplitude fluctuations resembling rapid eye movement-like activity. During these periods, there was also a decoupling between membrane potential and respiratory input. Although we did not monitor other possible sources of input to the olfactory system (for example, neuromodulatory systems) in these experiments, it is possible that these periods of decoupling

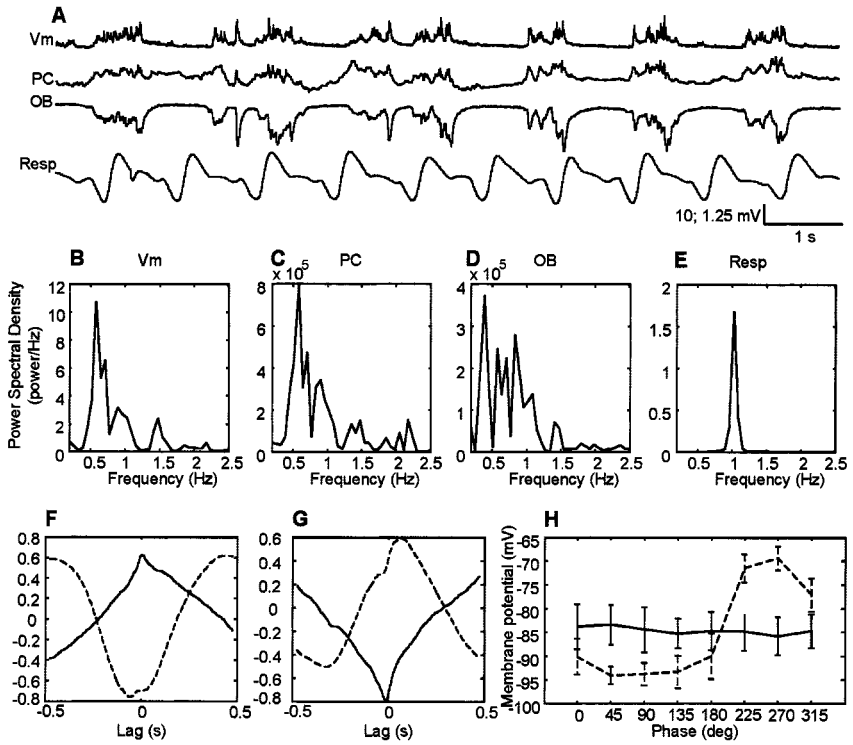

Figure 5. Comparisons of cortical, bulbar, and respiratory oscillations in tracheotomized rats. *A*, Raw traces of pyramidal cell membrane potential (Vm), local field potentials in layer I of PC, in the granule cell layer of the OB, and respiratory wave (Resp). In the respiratory wave, the downward deflection represents the inspiration. As in Figure 3, the graphs *B–E* indicate the power spectral density for the recorded membrane potentials (*B*), local field potentials recorded in piriform cortex (*C*), olfactory bulb (*D*), and ongoing respiration (*E*). *F*, Cross-covariance between membrane potential (Vm) of a layer II/III pyramidal cell and layer I olfactory cortex local field potentials. *G*, Cross-covariance between Vm and local field potentials in the granule cell layer of the olfactory bulb. *H*, Respiratory wave-triggered average of membrane potential. As in Figure 3*H*, the 0° phase represents the beginning of the inspiration. Dashed line, Intact preparation; continuous line, tracheotomized preparation.

result from other influences modifying the relationship between respiratory input and neural activity.

Afferent compared with intrinsic oscillatory mechanisms

Beyond the specific afferent signal or signals responsible for producing a correlation between inhalation and neural activity in the bulb and cortex, the results presented here also suggest that the contrast between extrinsic and intrinsic oscillatory mechanisms may be artificial. Although slow oscillations occur more regularly and at higher amplitude in the intact animals than in the tracheotomized animals, extracellular field potentials in the bulb and cortex, as well as intracellular membrane potentials in cortical pyramidal cells, continue to include activity at these frequencies, even in the absence of inhalation. Therefore, both the bulb and cortex appear to be capable of generating slow-frequency oscillations in the absence of periodic afferent input. However, afferent input clearly affects the coupling between the neuronal activity.

Perhaps the most surprising difference in neuronal coupling between the tracheotomized and intact preparations is the reversal of correlation between intracellular and extracellular recordings in the olfactory cortex. The association of positive field potentials with negative membrane potential in the intact animal is what one would expect from standard assumptions concerning current flow in cortical circuits (Ketchum and Haberly, 1993). The 180° shift in what has been thought to be a fundamental relationship in the tracheotomized animal was unexpected. Although current source–density analysis has demonstrated that reversals of this sort occur at different recording depths in the cortex (Ketchum and Haberly, 1993), we could shift these phase relationships back and forth with air puffs in the tracheotomized rat. Thus, this change would seem to reflect a fundamental difference in the organization of cortical activity between these two preparations. The change in correlation raises important questions regarding the relationship between intracellular- and extracellular-recorded activity, which will require additional experimental and network-modeling studies (Protopapas et al., 1998).

The influence of inhalation on slow oscillations in other regions of the olfactory-limbic axis

Given the influence of inhalation on neural activity in the olfactory bulb and cortex, we believe it is worth considering whether the temporal pattern of inhalation might also influence the periodic behavior of other forebrain structures. Within the olfactory-limbic axis, slow oscillations have been reported to occur in the entorhinal cortex (Biella et al., 2001), perirhinal cortex, and lateral amygdala (Collins et al., 1999; Collins et al., 2001). Although often considered separate from the olfactory system, each of these structures does receive a substantial projection from olfactory structures, including the olfactory bulb (Haberly, 1998). Although there is evidence in subcortical areas for the influence of other descending systems on oscillations (Steriade, 2001), at present, it is not known what if any role the olfactory system might play in generating or modulating slow oscillations in the limbic system. Our findings suggest that it might be fruitful to examine these oscillations with respect to respiration.

Relationship to neocortical slow oscillations

Slow oscillations, similar to those demonstrated here to occur in olfactory cortex, are also a stereotyped phenomenon present throughout the neocortex that has been recorded in visual, motor, and association areas (Steriade et al., 1993a). From a functional point of view, the neocortical slow oscillation has been interpreted as a state of sensory deafferentation of the cortex (Steriade, 2000). Our finding that the temporal structure of slow oscillations in the olfactory system is related to air entering the nostrils supports the view that slow oscillations seen in the olfactory system under ketamine–xylazine anesthesia are associated with periodic sensory input at the same frequencies. Our data therefore suggest that the slow oscillation in the olfactory system does not represent a state of deafferentation from the sensory input. To conclusively generalize the conclusions obtained in the olfactory system under ketamine–xylazine anesthesia to the sleep state, additional experiments will be necessary. Unfortunately, we are aware of no full study of olfactory bulbar or olfactory cortical activity during actual sleep; although, Freeman briefly noted that sleep was associated with an irregular slow-wave behavior that did not appear to be correlated with respiration (Freeman, 1959).

We suggested previously, on structural and computational

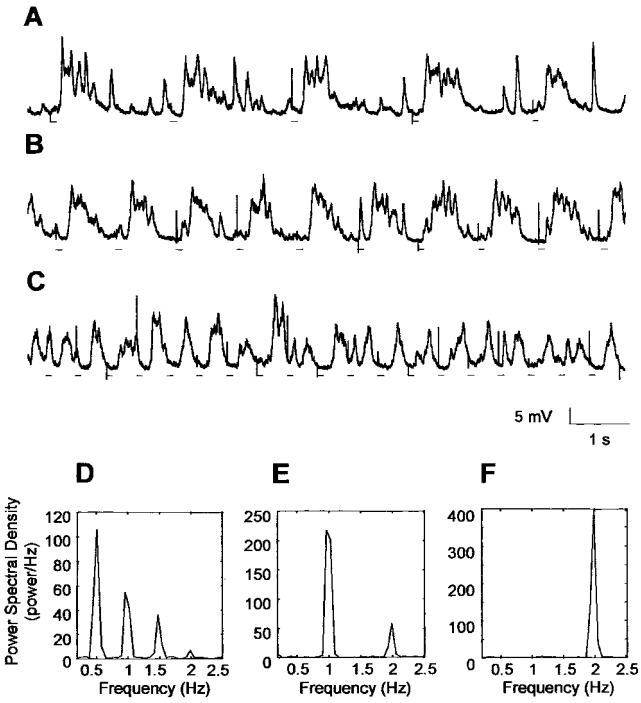

Figure 6. Air forced in the nostrils produces slow membrane potential fluctuations. Air pulses (black lines under traces) of 100 msec duration and 45 psi intensity were forced into the nostrils of the rat at different frequencies [~0.5 Hz (*A*), ~1 Hz (*B*), ~2 Hz (*C*)] when the rat was deeply anesthetized. The spiky depolarizations observed are electrical artifacts synchronized with the beginning of the air puff. *D*, *E*, and *F* show the peak in the power spectrum corresponding to the frequencies of air-induced oscillations.

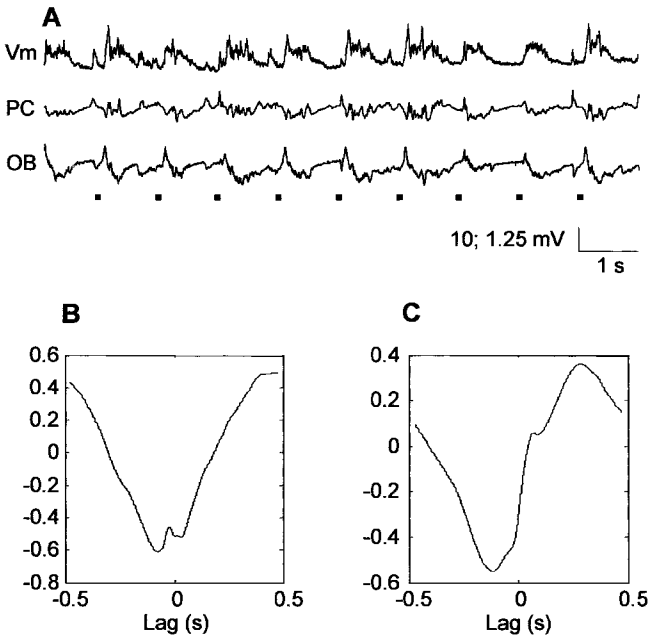

Figure 7. Effects of air forced in the nostrils on cross-covariance patterns. Air forced in the nostrils produces activity and cross-covariance patterns similar to those present in deeply anesthetized, freely breathing rats. *A*, Air puff-induced oscillations: Vm, membrane potential; PC piriform cortex local field potentials; OB, olfactory bulb local field potentials. Black lines represent the timing of the occurrence of air puffs. *B*, Representative cross-covariance between membrane potential and piriform cortex local field potentials. *C*, Representative cross-covariance between membrane potential and olfactory bulb local field potentials.

grounds, that the fundamental neuronal architecture of the cerebral cortex perhaps first evolved in the context of the olfactory system and was then adapted for the use of other sensory systems through the evolution of neocortex (Wilson and Bower, 1991, 1992; Bower, 1995; Morrissette and Bower, 1996). As part of that adaptation, we speculated that thalamocortical sensory pathways may have had to adapt to pattern neuronal activity into the dynamic frequencies native to the olfactory system (e.g., θ, γ). The results of this study suggest that the oscillatory activity patterns generated in the thalamo-neocortical system in the sleep state (Bazhenov et al., 2002) may also mimic the slow periodic inputs generated by the resting respiratory rhythm in the olfactory system. The essential point and prediction is that proper function of cortical circuitry during sleep, whatever that function is (Wilson and McNaughton, 1994; Lee and Wilson, 2002), requires or expects such slow periodic input because of an evolutionary link between cortical circuitry and olfaction.

References

Achermann P, Borbély AA (1997) Low-frequency (<1 Hz) oscillations in the human sleep electroencephalogram. Neuroscience 81:213–222.

Adrian ED (1942) Olfactory reactions in the brain of the hedgehog. J Physiol (Lond) 100:459–473.

Amzica F, Steriade M (1997) The K-complex: its slow (<1-Hz) rhythmicity and relation to delta waves. Neurology 49:952–959.

Bazhenov M, Timofeev I, Steriade M, Sejnowski TJ (2002) Model of thalamocortical slow-wave sleep oscillations and transitions to activated states. J Neurosci 22:8691–8704.

Bhalla US, Bower JM (1997) Multiday recordings from olfactory bulb neurons in awake freely moving rats: spatially and temporally organized variability in odorant response properties. J Comput Neurosci 4:221–256.

Biella GR, Dickson CT, De Curtis M (2001) Slow periodic activity in rhinal cortices of the isolated guinea pig brain preparation. Soc Neurosci Abstr 27:847.14.

Bower JM (1995) Reverse engineering the nervous system: an *in vivo*, *in vitro*, and *in computo* approach to understanding the mammalian olfactory system. In: An introduction to neural and electronic networks, Ed 2 (Zornetzer S, Davis J, Lau C, eds), pp 3–28. New York: Academic Press.

Bremer F (1958) Cerebral and cerebellar potentials. Physiol Rev 38:357–388.

Bressler SL (1984) Spatial organization of EEGs from olfactory bulb and cortex. Electroencephalogr Clin Neurophysiol 57:270–276.

Bressler SL, Freeman WJ (1980) Frequency analysis of olfactory system EEG in cat, rabbit, and rat. Electroencephalogr Clin Neurophysiol 50:19–24.

Buzsaki G (1998) Memory consolidation during sleep: a neurophysiological perspective. J Sleep Res 7:17–23.

Chaput MA (2000) EOG responses in anesthetized freely breathing rats. Chem Senses 25:695–701.

Chaput MA, Buonviso N, Berthommer F (1992) Temporal patterns in spontaneous and odour-evoked mitral cell discharges recorded in anesthetized freely breathing animals. Eur J Neurosci 4:813–822.

Collins ER, Lang EJ, Pare D (1999) Spontaneous activity of the perirhinal cortex in behaving cats. Neuroscience 89:1025–1039.

Collins DR, Pelletier JG, Pare D (2001) Slow and fast (gamma) neuronal oscillations in the perirhinal cortex and lateral amygdala. J Neurophysiol 85:1661–1672.

Destexhe A, Sejnowski TJ (2001) Thalamocortical assemblies. In: Monographs of the Physiological Society, Vol. 49. New York: Oxford UP.

Destexhe A, Contreras D, Steriade M (1999) Spatiotemporal analysis of local field potentials and unit discharges in cat cerebral cortex during natural wake and sleep states. J Neurosci 19:4595–4608.

Eckhorn R, Bauer R, Jordan W, Brosch M, Kruse W, Munk M, Reitboeck HJ (1988) Coherent oscillations: a mechanism of feature linking in the visual cortex? Biol Cybern 60:121–130.

Engel AK, Fries P, Singer W (2001) Dynamic predictions: oscillations and synchrony in top-down processing. Nat Rev Neurosci 2:704–716.

Fontanini A, Vanier MC, Moore LE, Bower JM (2001) Membrane potential oscillations in piriform cortex pyramidal cells: *in vivo* intracellular and local field potential recordings. Soc Neurosci Abstr 27:726.5.

Freeman WJ (1959) Distribution in time and space of prepyriform electrical activity. J Neurophysiol 22:644–665.
Freeman WJ (1960) Correlation of electrical activity of prepyriform cortex and behavior in cat. J Neurophysiol 23:111–131.
Freeman WJ (2000) Neurodynamics: an exploration in mesoscopic brain dynamics. London: Springer.
Gray CM, Konig P, Engel AK, Singer W (1989) Oscillatory responses in cat visual cortex exhibit inter-columnar synchronization which reflects global stimulus properties. Nature 338:334–337.
Haberly LB (1973) Unitary analysis of opossum prepyriform cortex. J Neurophysiol 36:762–774.
Haberly LB (1998) Olfactory cortex. In: The synaptic organization of the brain (Shepherd GM, ed), pp 377–416. New York: Oxford UP.
Haberly LB, Bower JM (1984) Analysis of association fiber system in piriform cortex with intracellular recording and staining techniques. J Neurophysiol 51:90–112.
Hasselmo ME, Fransen E, Dickson C, Alonso AA (2000) Computational modeling of entorhinal cortex. Ann NY Acad Sci 911:418–446.
Hopfield JJ (1995) Pattern recognition computation using action potential timing for stimulus representation. Nature 376:33–36.
Ketchum KL, Haberly LB (1993) Membrane currents evoked by afferent fiber stimulation in rat piriform cortex. I. Current source-density analysis. J Neurophysiol 69:248–260.
Lee AK, Wilson MA (2002) Memory of sequential experience in the hippocampus during slow wave sleep. Neuron 36:1183–1194.
Macrides F, Chorover SL (1972) Olfactory bulb units: activity correlates with inhalation cycles and odor quality. Science 175:84–87.
Morissette J, Bower JM (1996) Contribution of somatosensory cortex to responses in the rat cerebellar granule cell layer following peripheral tactile stimulation. Exp Brain Res 109:240–250.
Paxinos G, Watson C (1997) The rat brain in stereotaxic coordinates, Ed 3. San Diego: Academic.
Protopapas AD, Vanier MC, Bower JM (1998) Simulating large networks of neurons. In: Methods in neuronal modeling: from ions to networks (Koch C, Segev I, eds), pp 461–498. Cambridge, MA: MIT.
Sanchez-Vives MV, McCormick DA (2000) Cellular and network mechanisms of rhythmic recurrent activity in neocortex. Nat Neurosci 3:1027–1034.
Sobel EC, Tank DW (1993) Timing of odor stimulation does not alter patterning of olfactory bulb unit activity in freely breathing rats. J Neurophysiol 69:1331–1337.
Sobel N, Prabhakaran V, Desmond JE, Glover GH, Goode RL, Sullivan EV, Gabrieli JD (1998) Sniffing and smelling: separate subsystems in the human olfactory cortex. Nature 392:282–286.
Steriade M (2000) Corticothalamic resonance, states of vigilance and mentation. Neuroscience 101:243–276.
Steriade M (2001) Impact of network activities on neuronal properties in corticothalamic systems. J Neurophysiol 86:1–39.
Steriade M, Nunez A, Amzica F (1993a) A novel slow (<1 Hz) oscillation of neocortical neurons *in vivo*: depolarizing and hyperpolarizing components. J Neurosci 13:3252–3265.
Steriade M, Nunez A, Amzica F (1993b) Intracellular analysis of relations between the slow (<1 Hz) neocortical oscillation and other sleep rhythms of the electroencephalogram. J Neurosci 13:3266–3283.
Steriade M, Timofeev I, Grenier F (2001) Natural waking and sleep states: a view from inside neocortical neurons. J Neurophysiol 85:1969–1985.
Stripling JS, Patneau DK (1999) Potentiation of late components in olfactory bulb and piriform cortex requires activation of cortical association fibers. Brain Res 841:27–42.
Timofeev I, Steriade M (1996) Low-frequency rhythms in the thalamus of intact-cortex and decorticated cats. J Neurophysiol 76:4152–4168.
Timofeev I, Contreras D, Steriade M (1996) Synaptic responsiveness of cortical and thalamic neurones during various phases of slow sleep oscillation in cat. J Physiol (Lond) 494:265–278.
Timofeev I, Grenier F, Bazhenov M, Sejnowski TJ, Steriade M (2000) Origin of slow cortical oscillations in deafferented cortical slabs. Cereb Cortex 10:1185–1199.
Traub RD, Jeffreys GR, Whittington MA (1999) Fast oscillations in cortical circuits. Cambridge, MA: MIT.
Tsubone H (1990) Nasal 'pressure' receptors. Nippon Juigaku Zasshi 52:225–232.
Wehr M, Laurent G (1996) Odour encoding by temporal sequences of firing in oscillating neural assemblies. Nature 384:162–166.
Wilson D (1998) Habituation of odor responses in the rat anterior piriform cortex. J Neurophysiol 79:1425–1440.
Wilson M, Bower JM (1992) Cortical oscillations and temporal interactions in a computer simulation of piriform cortex. J Neurophysiol 67:981–995.
Wilson MA, Bower JM (1991) A computer simulation of oscillatory behavior in primary visual cerebral cortex. Neural Comput 3:498–509.
Wilson MA, McNaughton BL (1994) Reactivation of hippocampal ensemble memories during sleep. Science 265:676–679.